#100

J. Phys. Chem. Solids Vol. 46, No. 2, pp. 253–263, 1985
Printed in the U.S.A.

Papers from the
GEOPHYSICAL LABORATORY
Carnegie Institution of Washington
No. 1943

0022-3697/85 $3.00 + .00
Pergamon Press Ltd.

# HIGH-PRESSURE CRYSTAL CHEMISTRY OF SCHEELITE-TYPE TUNGSTATES AND MOLYBDATES

ROBERT M. HAZEN and LARRY W. FINGER
Geophysical Laboratory, Carnegie Institution of Washington, Washington, D.C. 20008, U.S.A.

and

JOSEPH W. E. MARIATHASAN
Clarendon Laboratory, Oxford University, Parks Road, Oxford OX1 3PU, England

(*Received* 30 *May* 1984; *accepted in revised form* 25 *July* 1984)

**Abstract**—Unit-cell parameters and crystal structures of $CaWO_4$ (scheelite) and $CaMoO_4$ (powellite) have been determined at several pressures to 5.8 GPa; and unit-cell parameters of $PbMoO_4$ (wulfenite), $PbWO_4$ (stolzite) and $CdMoO_4$ have been measured at pressures to 6.0 GPa. All five tetragonal scheelite-type compounds compress anisotropically, with the *c* axis 1.2 to 1.9 times more compressible than *a*. In both $CaWO_4$ and $CaMoO_4$ the cation tetrahedra (with $W^{6+}$ or $Mo^{6+}$) behave as rigid structural elements with no observed cation-oxygen compression (W—O and Mo—O bond compression < 0.001 $GPa^{-1}$). Compression of the eight-coordinated calcium polyhedron, on the other hand, is comparable to bulk compression of the compounds (Ca—O bond compression = 0.005 ± 0.001 $GPa^{-1}$). Anisotropies in the pressure response of the calcium polyhedron, which is more compressible parallel to *c* than perpendicular to *c*, result in the anisotropic unit-cell compression. Bulk moduli of the five compounds (with $K'$ assumed to be 4) are $CaWO_4$ (68 ± 9 GPa), $CaMoO_4$ (81.5 ± 0.7 GPa), $PbWO_4$ (64 ± 2 GPa), $PbMoO_4$ (64 ± 2 GPa), and $CdMoO_4$ (104 ± 2 GPa). No reversible transitions to the monoclinic (fergusonite) distortion of scheelite were observed in these compounds. Pressure–volume data for $PbWO_4$, however, display strong positive curvature ($K'_{calc}$ = 23 ± 2) up to about 5 GPa, at which pressure crystals appear to undergo a first-order phase transition. The relatively large curvature may be a premonitory effect prior to a reconstructive transition. Structural changes in these compounds with increasing pressure are qualitatively similar to changes that result from isobaric cooling or substitution of a smaller cation in the eight-coordinated site.

## INTRODUCTION

Scheelite-type $ABO_4$ compounds, with eight-coordinated *A* cations and tetrahedral *B* cations, are common binary oxides in both natural and synthetic systems. The scheelite structure is very versatile and occurs with +1, +2, +3 and +4 *A* cations in combination with +7, +6, +5 and +4 *B* cations, respectively. Solid solutions based on coupled, mixed-valence substitution and nonstoichiometric varieties such as $La_{0.7}MoO_4$ are also known.

Tungstates, molybdates, niobates and vanadates with the scheelite structure have been the focus of recent studies at high temperature and high pressure because of the identification of several phase transitions in these compounds. Nicol and Durana [1] measured high-pressure Raman spectra of $CaWO_4$ and $CaMoO_4$ in a solid-media apparatus in which NaCl was used as the pressure medium. Single-crystal specimens were aligned with the tetragonal *c* axis both parallel and perpendicular to the uniaxial stress of the experimental system. In both orientations, splitting of $E_g$ modes was observed at pressures above 2 GPa. This behavior was interpreted as evidence for a transition from the tetragonal scheelite structure (space group $I4_1/a$) to the closely related, but topologically distinct, wolframite structure (monoclinic, $P2/c$). A similar high-pressure Raman study of $SrWO_4$ by Ganguly and Nicol [2] also revealed splitting of $E_g$ modes above 2 GPa. Subsequent high-pressure Raman spectroscopy with polycrystalline $CaWO_4$ and $CaMoO_4$ in opposed-anvil devices by Breitinger *et al.* [3] and Jayaraman *et al.* [4], however, showed no evidence for such transitions. It appears from the opposed-anvil experiments that there are no high-pressure transitions in hydrostatically compressed $CaWO_4$ or $CaMoO_4$ below 3 GPa.

Raman mode splittings of the type reported by Nicol and Durana could result from a reversible transition from tetragonal scheelite to the monoclinic fergusonite structure (space group $I2/a$), which is displayed by several rare earth niobates and $BiVO_4$ [5, 6]. Raman spectra of monoclinic $LaNbO_4$ by Wada *et al.* [5] display two $B_g$ modes in the room-temperature, low-symmetry phase; these modes converge to an $E_g$ mode at about 480°C, where $LaNbO_4$ transforms reversibly to the undistorted scheelite form. Furthermore, under room conditions of temperature and pressure, compounds along the solid solution join $LaNbO_4$—$CaWO_4$ are monoclinic for lanthanum-rich compositions but approach tetragonal symmetry with increasing calcium content and achieve the ideal scheelite structure at about 40% $CaWO_4$ component [7]. It is not unreasonable to expect, therefore, that $CaWO_4$ might undergo a distortional

transition to the fergusonite structure either in the presence of shear or at high pressure.

Recently Jayaraman [8] has observed the appearance of several new bands in the Raman spectra of $PbWO_4$ and $PbMoO_4$ at about 5.0 and 9.0 GPa, respectively. These changes in vibration modes, in contrast to the simple splittings of bands in the scheelite-to-fergusonite transition, imply a first-order phase transition.

The objectives of this high-pressure crystallographic study of scheelite-type tungstates and molybdates are to:

(1) document and characterize any phase transitions in $CaWO_4$ (scheelite), $CaMoO_4$ (powellite), $PbWO_4$ (wulfenite), $PbMoO_4$ (stolzite) and $CdMoO_4$ to pressures above 5 GPa;

(2) determine pressure–volume equation-of-state parameters for these five compounds; and

(3) determine high-pressure crystal structures in order to define relationships between bonding and compression of scheelite-type compounds.

## EXPERIMENTAL

### *Specimen description*

Crystals of $CaWO_4$, $CaMoO_4$ and $CdMoO_4$ were provided by John S. White from the synthetic compounds collection of the National Museum of Natural History, Smithsonian Institution (specimen numbers 148668, 148773 and 51S, respectively). Both $CaWO_4$ and $CdMoO_4$ were synthesized at Bell Laboratories, whereas the $CaMoO_4$ was synthesized by Isomet Corporation. Crystal fragments of $PbWO_4$ and $PbMoO_4$ were supplied by A. Jayaraman from material synthesized at Bell Laboratories.

All five synthetic scheelite-type compounds were obtained as fragments from colorless boules of near-ideal compositions. Exact conditions of sample preparation were not specified, but room-condition unit-cell parameters match those reported for end-member material [9].

### *Data collection at room pressure*

Single-crystal diffraction data were collected on rectangular cleavage fragments with a 60-$\mu$m maximum dimension for Ca and Cd compounds and a 40-$\mu$m maximum dimension for the highly absorbing Pb compounds. Room-temperature lattice parameters for each of the five compounds were refined from diffractometer angles of 20 reflections, each of which was measured in eight equivalent positions [10]. Unit-cell parameters are recorded in Table 1.

Crystal-structure refinements at room and high pressure were performed on $CaWO_4$ and $CaMoO_4$. All scheelite-type tungstates and molybdates have relatively large linear absorption coefficients and thus may be subject to systematic errors in X-ray data. The calcium compounds were selected for crystal-structure analysis both because of their mineralogical interest and because they have lower X-ray absorption than many other scheelite-type crystals. Intensities of all reflections in a sphere with $(\sin\Theta)/\lambda \leqq 0.7$ were measured by an automated, four-circle diffractometer with Nb-filtered Mo$K\alpha$ radiation [11].

Refinement conditions and refined structural parameters for $CaWO_4$ and $CaMoO_4$ appear in Table 2; the refined anisotropic temperature factors under room conditions are presented in Table 3.

### *Data collection at high pressure*

Flat cleavage plates from 10 $\mu$m (for Pb compounds) to 50 $\mu$m thick and from 50 to 100 $\mu$m in diameter were employed in high-pressure experiments. Crystals were mounted in a diamond-anvil pressure cell for X-ray diffraction [12]. An alcohol mixture of 4:1 methanol:ethanol was used as the hydrostatic pressure medium [13], and ruby crystals were included in each mount for pressure calibration [14]. Details of procedures for crystal mounting and high-pressure X-ray diffraction are described elsewhere [12].

Lattice constants of all five scheelite-type compounds were measured at several pressures. From 10 to 20 reflections were measured by the method of Hamilton [15], as modified by King and Finger [10], in order to correct for errors in crystal centering and diffractometer alignment. Each set of angular data was refined without constraint, and the resulting "triclinic" cell was examined for conformity with the tetragonal symmetry of scheelite. These symmetry conditions (i.e. $a = b$ and $\alpha = \beta = \gamma = 90°$) are satisfied within two standard deviations for all compounds at all pressures studied. The uniaxial behavior observed is evidence that no deviations from tetragonal symmetry occurred and, furthermore, that hydrostatic conditions were maintained during the experiments. High-pressure unit-cell parameters are recorded in Table 1 and are illustrated for the calcium and lead scheelites in Figs. 1 and 2, respectively.

Intensity data for three-dimensional structure refinements were collected for the two calcium compounds; all accessible reflections with $(\sin\Theta)/\lambda \leqq 0.7$ were measured.* The fixed-$\phi$ mode of data collection was used to maximize reflection accessibility and minimize attenuation by the diamond cell [16], and a correction was made for X-ray absorption by the diamond and beryllium components of the pressure cell [12]. Conditions of high-pressure refinements as well as refined structure parameters are recorded in Table 2.

Refined high-pressure structure parameters for $CaMoO_4$ were consistent with those determined at room pressure. High-pressure parameters for $CaWO_4$, however, varied systematically from the room-pressure values (Table 2). It was necessary, therefore, to collect a room-pressure data set from the high-pressure crystal in the pressure cell. This structure refinement was used in subsequent calculations of bond compressions. The significant differences in room-

* Tabulated observed and calculated structure factors for all refinements are available from the authors on request.

Table 1. Unit-cell dimensions* of scheelite-type tungstates and molybdates at several pressures

| Specimen | Pressure (GPa) | a (A) | c (A) | V (A$^3$) | V/V$_0$ | c/a |
|---|---|---|---|---|---|---|
| $CaWO_4$ | 0.0001 | 5.2429(3)† | 11.3737(6) | 312.6(4) | 1.0000 | 2.169 |
| | 0.71(5) | 5.2266(6) | 11.323(1) | 309.3(7) | 0.9894 | 2.167 |
| | 1.03(5) | 5.2160(6) | 11.313(3) | 307.8(1) | 0.9846 | 2.169 |
| | 2.03(5) | 5.1936(4) | 11.255(2) | 303.6(1) | 0.9712 | 2.167 |
| | 3.12(5) | 5.174(3) | 11.197(5) | 299.7(1) | 0.9587 | 2.164 |
| | 4.09(5) | 5.160(3) | 11.142(4) | 296.7(1) | 0.9491 | 2.157 |
| $CaMoO_4$ | 0.0001 | 5.222(1) | 11.425(3) | 311.5(2) | 1.0000 | 2.188 |
| | 0.65(5) | 5.2116(3) | 11.395(8) | 309.5(2) | 0.9936 | 2.186 |
| | 1.30(5) | 5.1996(5) | 11.365(3) | 307.25(8) | 0.9864 | 2.186 |
| | 2.49(5) | 5.1801(3) | 11.301(2) | 303.25(6) | 0.9735 | 2.182 |
| | 2.75(5) | 5.1755(4) | 11.282(2) | 302.19(6) | 0.9701 | 2.180 |
| | 3.20(5) | 5.167(1) | 11.260(2) | 300.65(9) | 0.9652 | 2.179 |
| | 3.65(5) | 5.1605(9) | 11.226(4) | 299.0(1) | 0.9599 | 2.175 |
| | 4.19(5) | 5.1515(6) | 11.193(9) | 297.0(2) | 0.9535 | 2.173 |
| | 4.89(5) | 5.1402(5) | 11.162(3) | 294.92(9) | 0.9468 | 2.172 |
| | 5.10(5) | 5.138(1) | 11.152(2) | 294.40(7) | 0.9451 | 2.172 |
| | 5.71(5) | 5.1286(3) | 11.119(5) | 292.4(1) | 0.9387 | 2.168 |
| | 6.18(5) | 5.124(7) | 11.109(3) | 291.72(9) | 0.9365 | 2.168 |
| $CdMoO_4$ | 0.0001 | 5.1542(3) | 11.1926(7) | 297.34(3) | 1.0000 | 2.172 |
| | 0.80(5) | 5.1443(2) | 11.165(2) | 295.47(5) | 0.9937 | 2.170 |
| | 2.27(5) | 5.1245(1) | 11.101(2) | 291.53(4) | 0.9805 | 2.166 |
| | 3.71(5) | 5.1043(2) | 11.038(4) | 287.57(11) | 0.9671 | 2.162 |
| | 4.80(5) | 5.0907(2) | 10.992(2) | 284.87(6) | 0.9581 | 2.159 |
| $PbWO_4$ | 0.0001 | 5.4595(3) | 12.0432(7) | 358.96(3) | 1.0000 | 2.206 |
| | 0.69(5) | 5.436(1) | 11.957(2) | 353.43(18) | 0.9846 | 2.200 |
| | 1.41(5) | 5.4206(5) | 11.894(2) | 349.47(13) | 0.9736 | 2.194 |
| | 2.73(5) | 5.393(1) | 11.786(2) | 342.83(10) | 0.9551 | 2.185 |
| | 4.08(5) | 5.376(1) | 11.704(3) | 338.26(19) | 0.9423 | 2.177 |
| | 4.83(5) | 5.367(1) | 11.653(2) | 335.75(13) | 0.9353 | 2.171 |
| | 5.41(5) | 5.365(2) | 11.632(3) | 334.8(3) | 0.9327 | 2.168 |
| | 5.97(5) | 5.360(1) | 11.601(2) | 333.32(13) | 0.9286 | 2.164 |
| $PbMoO_4$ | 0.0001 | 5.4351(3) | 12.1056(8) | 357.60(3) | 1.0000 | 2.227 |
| | 0.38(5) | 5.420(3) | 12.062(13) | 354.2(4) | 0.9905 | 2.225 |
| | 1.03(5) | 5.404(1) | 12.002(2) | 350.6(1) | 0.9804 | 2.221 |
| | 1.47(5) | 5.398(1) | 11.969(3) | 348.7(2) | 0.9751 | 2.217 |
| | 1.98(5) | 5.388(1) | 11.941(3) | 346.7(1) | 0.9695 | 2.216 |
| | 2.59(5) | 5.385(1) | 11.892(4) | 344.8(2) | 0.9642 | 2.208 |
| | 4.07(5) | 5.356(1) | 11.791(3) | 338.4(2) | 0.9463 | 2.201 |
| | 5.34(5) | 5.334(1) | 11.691(4) | 332.7(2) | 0.9304 | 2.192 |

*Unit-cell dimensions were refined from diffractometer data without constraint (i.e., as triclinic). For all measurements a = b and $\alpha = \beta = \gamma = 90^\circ$ within 2σ.

†Parenthesized figures represent esd's.

pressure parameters of $CaWO_4$ in and out of the pressure cell are probably the result of systematic absorption errors caused by the large linear absorption coefficient of calcium tungstate ($\mu_l$ = 384 cm$^{-1}$), combined with the limited access to reciprocal space, which is typical of diamond-cell experiments. Although absolute values of bond distances are not well defined, comparisons can be made between the several $CaWO_4$ high-pressure refinements because all of them are subject to the same systematic errors.

## RESULTS

### *Linear compressibilities and bulk moduli*

Linear compressibilities and equation-of-state parameters have been calculated from unit-cell data in Table 1 and are summarized in Table 4. Unit-cell edges $a$ and $c$ may be expressed as functions of pressure:

$$a = a_0 - d_1P + d_2P^2.$$

Cell edge compressibilities of $CaMoO_4$ and $CdMoO_4$ are linear so that only the $d_1$ terms are required. The other three compounds, however, display marked positive curvature in pressure-cell edge data so $d_2$ is significant for $CaWO_4$, $PbWO_4$ and $PbMoO_4$ (Figs. 1 and 2; Table 4). All of these scheelite-type compounds compress anisotropically, with $c$ from 1.2 to 1.9 times more compressible than $a$.

Bulk modulus, $K_0$, and its pressure derivative, $K'$, were calculated from pressure–volume data by least-squares procedures. Bulk moduli were first calculated

Table 2. Refinement conditions and refined structural parameters for $CaWO_4$ and $CaMoO_4$ at high pressure

| Specimen | Pressure (GPa) | Weighted $\underline{R}$ (%)† | $\underline{R}$ (%)‡ | No. of Observations§ | $\underline{X}_0$ | $\underline{Y}_0$ | $\underline{Z}_0$ | $\underline{B}_{Ca}$ | $\underline{B}_R^{6+}$ | $\underline{B}_0$ | $\underline{r}^*$ ($\times 10^5$) |
|---|---|---|---|---|---|---|---|---|---|---|---|
| $CaWO_4$ | 0.0001 | 2.2 | 2.3 | 197 | 0.1507(9) | 0.0086(10) | 0.2106(4) | 0.58(6) | 0.44(3) | 0.68(12) | 3.3(2) |
| $\mu_\ell$=384.3 $cm^{-1}$ | 0.0001 (in cell) | 2.2 | 2.5 | 63 | 0.1488(20) | 0.0038(20) | 0.2159(25) | 1.16(11) | 0.75(6) | 1.39(21) | 4.1(5) |
| | 1.03(5) | 2.1 | 2.2 | 60 | 0.1493(18) | 0.0049(18) | 0.2158(23) | 1.09(9) | 0.75(5) | 1.19(18) | 0.4(2) |
| | 2.03(5) | 2.2 | 2.7 | 63 | 0.1523(17) | 0.0045(17) | 0.2179(21) | 1.06(9) | 0.82(4) | 1.27(17) | 0.3(2) |
| | 3.12(5) | 2.6 | 3.1 | 60 | 0.1518(20) | 0.0047(21) | 0.2183(26) | 1.07(11) | 0.75(5) | 0.99(21) | 0.1(1) |
| | 4.09(5) | 2.2 | 2.4 | 58 | 0.1534(19) | 0.0009(21) | 0.2153(26) | 1.17(10) | 0.83(5) | 1.45(21) | 0.1(1) |
| $CaMoO_4$ | 0.0001 | 2.1 | 2.5 | 175 | 0.1490(6) | 0.0069(6) | 0.2089(3) | 0.88(3) | 0.77(2) | 1.02(5) | 1.6(5) |
| $\mu_\ell$=55.3 $cm^{-1}$ | 1.30(5) | 2.7 | 3.7 | 91 | 0.1503(11) | 0.0051(11) | 0.2094(11) | 0.90(5) | 0.45(5) | 0.90(11) | 6.1(7) |
| | 2.49(5) | 2.2 | 2.1 | 71 | 0.1516(6) | 0.0056(6) | 0.2089(8) | 1.00(4) | 0.77(3) | 1.09(6) | 1.8(2) |
| | 3.65(5) | 2.6 | 2.6 | 66 | 0.1536(7) | 0.0052(6) | 0.2110(9) | 0.86(4) | 0.68(4) | 1.03(7) | 1.7(2) |
| | 4.19(5) | 2.6 | 2.8 | 80 | 0.1541(11) | 0.0048(11) | 0.2109(11) | 0.80(5) | 0.47(5) | 0.82(11) | 4.9(6) |
| | 5.10(5) | 3.3 | 4.3 | 90 | 0.1584(13) | 0.0060(13) | 0.2121(13) | 0.81(7) | 0.20(5) | 0.67(11) | 0.6(1) |
| | 5.71(5) | 3.2 | 3.4 | 74 | 0.1580(15) | 0.0075(15) | 0.2115(15) | 0.90(8) | 0.17(5) | 0.75(16) | 0.2(1) |

†Weighted $\underline{R} = [\Sigma w(|Fo| - |Fe|)^2/\Sigma wFo^2]^{1/2}$.

‡$\underline{R} = \Sigma[|Fo| - |Fe|]/\Sigma|Fo|$.

§Symmetrically equivalent reflections have been averaged. A reflection is observed if $\underline{I} \geq 2\sigma_{\underline{I}}$.

Table 3. Anisotropic thermal parameters for $CaWO_4$ and $CaMoO_4$ at room pressure

| Compound | Atom | $\beta_{11}$ | $\beta_{22}$ | $\beta_{33}$ | $\beta_{12}$ | $\beta_{13}$ | $\beta_{23}$ |
|---|---|---|---|---|---|---|---|
| $CaWO_4$ | Ca | 0.0041(5)* | 0.0041(5) | 0.0015(2) | 0.0 | 0.0 | 0.0 |
| | W | 0.0032(2) | 0.0032(2) | 0.0013(1) | 0.0 | 0.0 | 0.0 |
| | O | 0.0067(17) | 0.0059(15) | 0.0018(3) | 0.0012(13) | 0.0007(6) | 0.0007(6) |
| $CaMoO_4$ | Ca | 0.0082(3) | 0.0082(3) | 0.0016(1) | 0.0 | 0.0 | 0.0 |
| | Mo | 0.0066(2) | 0.0066(2) | 0.0017(1) | 0.0 | 0.0 | 0.0 |
| | O | 0.0091(11) | 0.0012(11) | 0.0020(2) | 0.0016(8) | -0.0001(4) | 0.0015(4) |

*Parenthesized figures represent esd's.

with a first-order Birch–Murnaghan equation of state based on the assumption that $K' = 4$ [12]. The two lead compounds ($K = 64 \pm 2$ GPa) are the most compressible, whereas $CdMoO_4$ ($K = 104 \pm 2$ GPa) is the least compressible. The calcium tungstate and molybdate ($K = 68 \pm 9$ and $82 \pm 1$ GPa, respectively) have intermediate values. Note that static measurements of the bulk moduli and linear compressibilities for $CaMoO_4$, $CaWO_4$ and $PbMoO_4$ are in good agreement with values determined by ultrasonic techniques [17].

A first-order Birch–Murnaghan equation of state does not adequately model pressure–volume data for $CaWO_4$ and the two lead compounds, which display relatively strong positive curvature (Figs. 1 and 2). The pressure–volume data were thus used to calculate both $K_0$ and $K'$ with a second-order Birch–Murnaghan equation of state [12]. Values of the pressure derivative of bulk modulus (Table 4) are within the normal range for three of the five compounds. The calculated $K'$ for $CdMoO_4$ ($K' = -2 \pm 2$) is negative, but only five pressure–volume data are available and the negative curvature is not significant. The $K'$ for $PbWO_4$ ($K' = 23 \pm 2$) is anomalously large. It is possible that the unusual "stiffening" of lead tungstate below 5 GPa is premonitory to the first-order phase transition observed with Raman spectroscopy. It should be noted, however, that the extremely high linear absorption coefficient of $PbWO_4$ ($\mu_l = 780$ cm$^{-1}$) makes

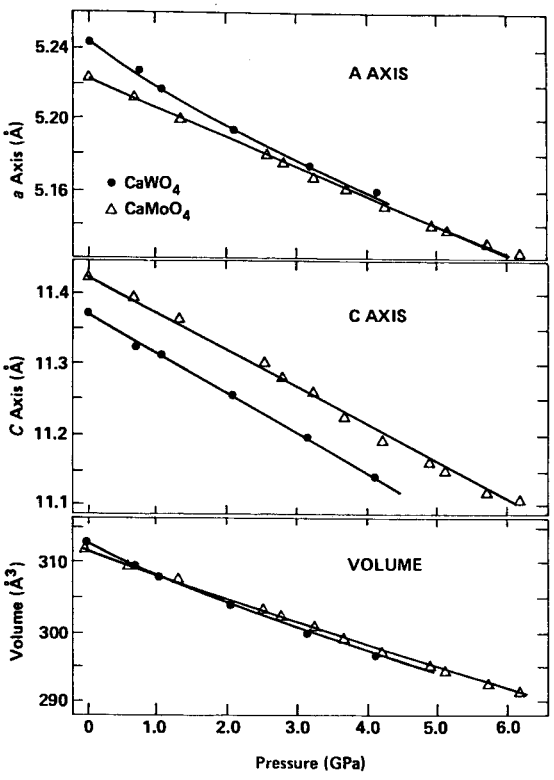


Fig. 1. Unit-cell parameters of $CaWO_4$ and $CaMoO_4$ versus pressure.

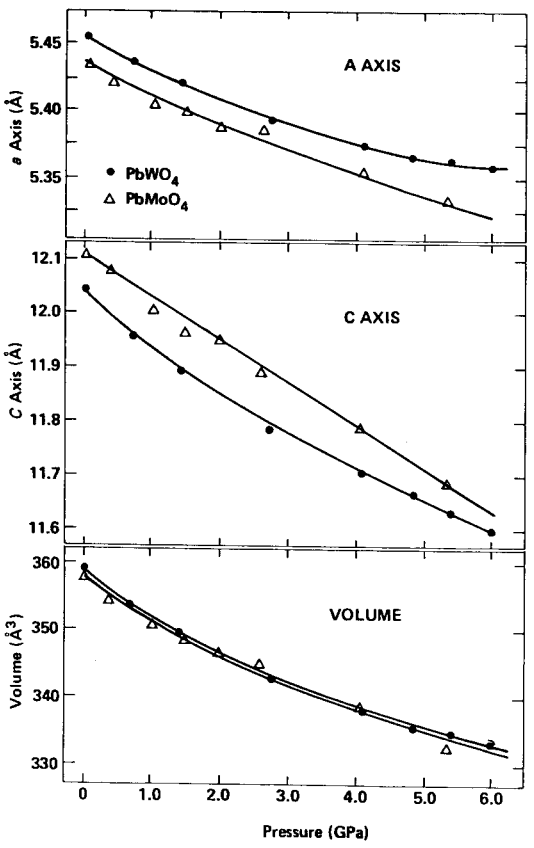


Fig. 2. Unit-cell parameters of $PbWO_4$ and $PbMoO_4$ versus pressure.

Table 4. Linear compressibilities and bulk moduli for scheelite-type tungstates and molybdates

| Compound | Axis | $\ell_0$ (Å) | $d_1$ ($GPa^{-1}$) | $d_2$ ($GPa^{-1}$) | $\bar{\beta}_\ell$* ($\times 10^3$ $GPa^{-1}$) | $\bar{\beta}_{\parallel} / \bar{\beta}_{\perp}$ | $\bar{\beta}_V$* | $K_0$† (GPa) | K'† |
|---|---|---|---|---|---|---|---|---|---|
| $CaWO_4$ | a | 5.2431(7)‡ | 0.027(1) | 0.0015(6) | 4.3(1) | 1.2 | 0.014 | 68(9) | 4† |
| | c | 11.373(2) | 0.067(5) | 0.003(2) | 5.2(2) | | | 61(10) | 10(1) |
| $CaMoO_4$ | a | 5.2231(4) | 0.0164(1) | -- | 3.14(3) | 1.50 | 0.011 | 81.5(7) | 4† |
| | c | 11.430(4) | 0.0538(9) | -- | 4.70(8) | | | 88(2) | 2(1) |
| $PbWO_4$ | a | 5.4593(6) | 0.0307(8) | 0.0024(2) | 3.4(3) | 1.9 | 0.013 | 64(2) | 4† |
| | c | 12.042(2) | 0.112(4) | 0.0065(7) | 6.4(3) | | | 38(2) | 23(2) |
| $PbMoO_4$ | a | 5.435(1) | 0.025(2) | 0.0012(5) | 3.6(1) | 1.8 | 0.013 | 64(2) | 4† |
| | c | 12.105(3) | 0.093(5) | 0.0034(12) | 6.6(2) | | | 57(5) | 8(3) |
| $CdMoO_4$ | a | 5.1548(4) | 0.0134(2) | -- | 2.60(4) | 1.43 | 0.009 | 104(2) | 4† |
| | c | 11.193(1) | 0.0416(7) | -- | 3.72(5) | | | 117(4) | -2(2) |

*Mean compressibility between 1 bar and 5 GPa: $\bar{\beta} = \frac{\ell_0 - \ell_5}{5\ell_0}$ or $\bar{\beta}_V = \frac{V_0 - V_5}{5V_0}$.

†Equation-of-state parameters $K_0$ and K' are calculated from best fit of pressure-volume data to a Birch-Murnaghan equation of state.

‡Parenthesized figures represent esd's.

X-ray diffraction experiments difficult; systematic errors in unit-cell data cannot be ruled out.

### *High-pressure crystal structures*

Scheelite is tetragonal, space group $I4_1/a$, with four $CaWO_4$ molecules per unit cell. There are three symmetrically distinct atoms in the tetragonal scheelite structure. The Ca and W of scheelite are both on fixed special positions of site symmetry $\bar{4}$ at $(0, \frac{1}{4}, \frac{5}{8})$ and $(0, \frac{1}{4}, \frac{1}{8})$, respectively. (The conventional setting of the unit cell, with origin at $\bar{1}$ at $0, \frac{1}{4}, \frac{1}{8}$ from $\bar{4}$, is used throughout this study.) The oxygen atom is in the general position with approximate coordinates (0.15, 0.01, 0.21). The scheelite structure may be visualized in terms of its two constituent cation polyhedra, the eight-coordinated calcium site and the tetrahedral tungsten site. Each calcium site shares edges with four adjacent calcium sites and shares corners with eight adjacent tetrahedra (Fig. 3). Each tetrahedron is linked to eight calcium sites (two to each oxygen). The high-pressure behavior of scheelite-type compounds is perhaps best described in terms of the pressure response of these two polyhedra.

Tungsten and molybdenum tetrahedra in $CaWO_4$ and $CaMoO_4$ are rigid structural elements that undergo little, if any, change in size or shape with pressure to 6 GPa (Table 5, Fig. 4). This behavior is consistent with polyhedral bulk modulus–volume systematics developed by Hazen and Finger [19]. A simple relationship for predicting polyhedral bulk moduli of oxides is

$$K_p \text{ (in GPa)} = 750 Z_c / d^3,$$

where $Z_c$ is cation formal charge and $d$ is the mean cation–anion bond distance. For $W^{6+}$ and $Mo^{6+}$ tetrahedra, with mean $T$—O bond distances of about 1.8 Å, the predicted tetrahedral bulk modulus is approx. 800 GPa. This value is consistent with the observed tetrahedral bulk moduli, which are greater than 500 GPa. (For comparison, the bulk modulus of diamond is about 590 GPa [12].) The relative rigidity of the tungsten and molybdenum tetrahedra should result in any property dependent upon tetrahedral configuration (internal modes of vibration, for example) being independent of pressure.

Calcium—oxygen bond compression in both $CaWO_4$ and $CaMoO_4$ is significantly greater than compression of the respective tetrahedra; compressibility for the two symmetrically distinct Ca—O bonds in both compounds is consistent with a value of 0.005 $GPa^{-1}$ (Fig. 4; Table 6). The predicted polyhedral bulk modulus of the calcium site ($Z_c$ = 2; $d$ = 2.6 Å) is 80 GPa, which compares well with the observed value of 70 GPa.

The anisotropic compressibility of scheelite-type compounds may be understood by examining the eight-coordinated calcium site in detail. The eight-coordinated calcium site of $CaMoO_4$ at room pressure and at 5.7 GPa is illustrated in Fig. 5. Whereas all Ca—O bonds compress at approximately the same rate, the four distinct adjacent oxygen—oxygen bonds have slightly different compressibilities (Table 6). The height of the calcium site parallel to $c$ (line $C$–$C'$ on Fig. 5) compresses from 3.802 to 3.637 Å (4.3%), whereas the width of the polyhedron (line $A$–$A'$ on Fig. 5) compresses from 3.816 to 3.741 Å (2.0%). The lower compressibility of $A$–$A'$, which is manifest in the anisotropic unit-cell compression of scheelites, may be related to the orientation of shared edges between eight-coordinated sites. These short edges, represented by oxygen pairs 1–4, 2–3, 5–7 and 6–8 in Fig. 5, lie close to the (0 0 1) plane and may thus restrict compression perpendicular to $c$.

## CONCLUSIONS

### *Comparative crystal chemistry of scheelite*

The high-pressure behavior of scheelite-type compounds may be compared to behavior with changing temperature and changing eight-coordinated site

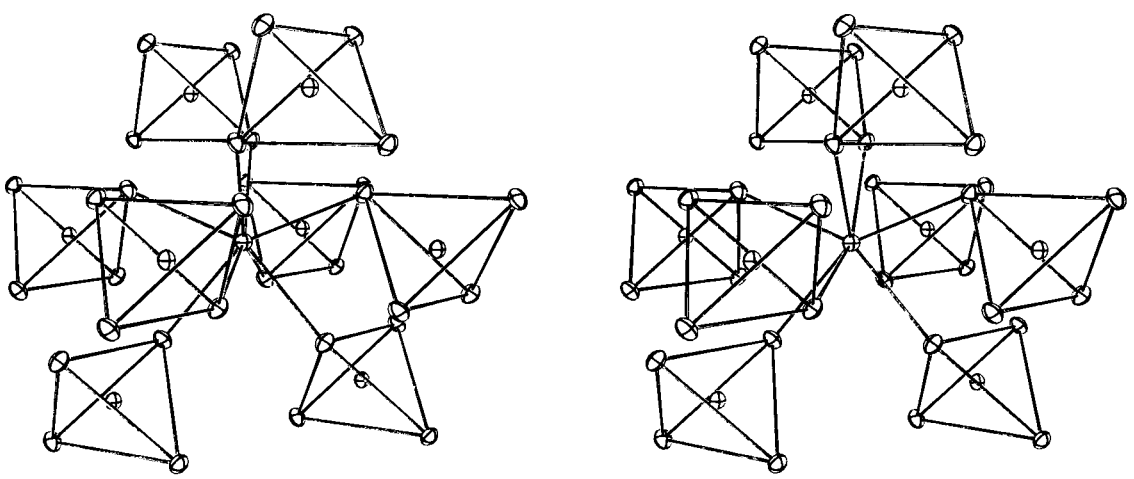

Fig. 3. A portion of the scheelite structure, illustrating the arrangement of tungsten tetrahedra surrounding the eight-coordinated calcium site.

Table 5. Tetrahedral bond distances, bond angles, volume, distortion indices, and compressibilities for $CaWO_4$ and $CaMoO_4$

| Specimen | Pressure (GPa) | T-O[4]* | O-O[4] | O-O[2] | O-T-O[4] | O-T-O[2] | Volume (Å$^3$) | Quadratic Elongation† | Angle Variance† |
|---|---|---|---|---|---|---|---|---|---|
| $CaWO_4$ | 0.0001 | 1.782(5)‡ | 2.871(8) | 2.984(10) | 107.4(2) | 113.8(3) | 2.89(1) | 1.003(2) | 11(1) |
| | 0.0001 in cell | 1.828(19) | 2.970(42) | 3.016(21) | 108.6(8) | 111.2(15) | 3.22(5) | 1.001(7) | 5(8) |
| | 1.03(5) | 1.815(17) | 2.950(39) | 2.994(19) | 108.7(7) | 111.1(14) | 3.07(4) | 1.000(6) | 2(7) |
| | 2.03(5) | 1.829(16) | 2.980(35) | 3.001(18) | 109.1(6) | 110.2(13) | 3.14(4) | 1.000(5) | 1(6) |
| | 3.12(5) | 1.822(19) | 2.970(40) | 2.985(21) | 109.2(2) | 110.0(15) | 3.10(5) | 1.000(7) | 0(5) |
| | 4.09(5) | 1.814(19) | 2.933(42) | 3.019(42) | 107.9(8) | 112.7(16) | 3.16(5) | 1.005(6) | 18(9) |
| | Compressibility ($GPa^{-1}$) | 0.002(3) | 0.005(6) | 0.000(5) | | | 0.002(7) | | |
| $CaMoO_4$ | 0.0001 | 1.771(3) | 2.848(5) | 2.977(6) | 107.1(1) | 114.4(2) | 2.83(1) | 1.004(1) | 15(1) |
| | 1.30(5) | 1.775(9) | 2.854(19) | 2.988(11) | 107.0(3) | 114.6(7) | 2.86(5) | 1.004(3) | 16(2) |
| | 2.49(5) | 1.766(6) | 2.835(13) | 2.979(6) | 106.8(2) | 115.0(5) | 2.81(1) | 1.005(2) | 18(2) |
| | 3.65(5) | 1.776(6) | 2.859(14) | 2.983(7) | 107.2(3) | 114.2(5) | 2.86(2) | 1.003(2) | 13(2) |
| | 4.19(5) | 1.775(9) | 2.854(19) | 2.984(12) | 107.1(3) | 114.4(7) | 2.85(2) | 1.004(3) | 15(2) |
| | 5.10(5) | 1.782(10) | 2.871(21) | 2.990(13) | 107.3(4) | 114.0(8) | 2.89(2) | 1.003(2) | 13(3) |
| | 5.71(5) | 1.768(11) | 2.847(24) | 2.969(15) | 107.2(4) | 114.1(9) | 2.83(3) | 1.003(4) | 13(3) |
| | Compressibility ($GPa^{-1}$) | -0.001(1) | -0.002(2) | -0.001(1) | | | -0.002(2) | | |

*Bracketed figures represent bond multiplicity.
†Quadratic elongation and bond-angle variance are polyhedral distortion parameters defined by Robinson et al.[18]. Values for a regular tetrahedron are 1.0 and 0.0, respectively.
‡Parenthesized figures represent esd's.

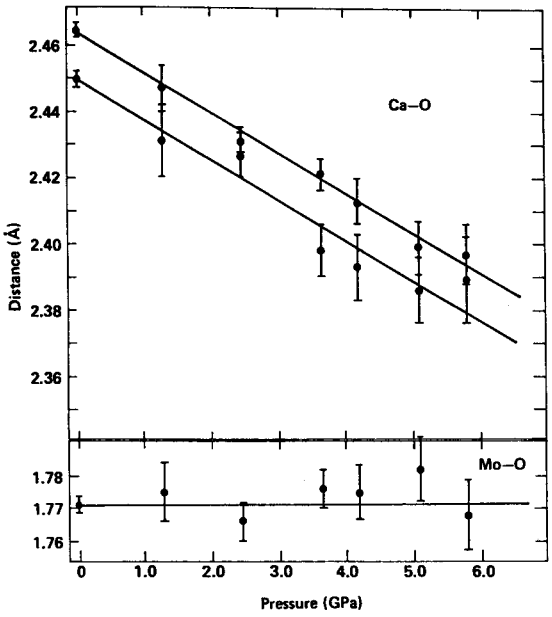


Fig. 4. Variation of Mo—O and Ca—O bond distances in $CaMoO_4$ vs pressure.

composition. No high-temperature structure refinements are available for scheelite-type tungstates or molybdates but aspects of high-temperature structures may be inferred from thermal expansion data. Deshpande and Suryanarayana [20] measured the thermal expansion of $CaMoO_4$ and summarized previous expansion data for other isomorphs. In all these compounds, including $CaWO_4$, $SrWO_4$, $CaMoO_4$ and $CdMoO_4$, the *c* axis is approx. twice as expandable as *a*. It can be assumed that the tungsten and molybdenum tetrahedra are invariant with temperature, so the principal structural changes upon heating are the anisotropic expansion of the eight-coordinated site. Scheelite compounds thus conform to the "inverse relationship" [12]; structural changes during isobaric heating are qualitatively opposite those during isothermal compression.

It is evident that the principal structural variations that occur with changes in temperature or pressure are associated with the large, eight-coordinated site. Similar structural changes may be caused by substitution of different cations in the large site. Consider the change in unit-cell parameters from $CdMoO_4$ to $CaMoO_4$ to $PbMoO_4$, which represents a change in eight-coordinated cation radius from 0.95 to 1.00 to 1.19 Å. The *a* axis increases from 5.154 to 5.222 to 5.435 Å (a total of 5.4%), whereas the *c* axis increases from 11.193 to 11.425 to 12.106 Å (8.2%). The *c*-axis coefficient of "compositional expansion" is significantly greater than that of the *a* axis. Similar behavior is exhibited by the tungstates. The change in unit-cell parameters between $CaWO_4$ and $PbWO_4$ is 4.1% in *a* and 5.9% in *c*.

Structural variations in the scheelite-type tungstates and molybdates are analogous, whether they are caused by changes in temperature, pressure, or composition. The size and shape of the W or Mo tetrahedron remains constant; the tetrahedron is a rigid, invariant structural unit. Significant structural changes occur, however, in the eight-coordinated site, which varies more parallel to *c* than perpendicular to *c* with changes in temperature, pressure, or composition.

### *Relative compressibility of scheelite-type compounds*

Mariathasan [21] measured the high-pressure structures and compressibilities of scheelite-type $BiVO_4$ and $LaNbO_4$ and observed structural behavior analogous to that of the scheelite-type tungstates and molybdates. In both of these $A^{3+}B^{5+}O_4$ compounds the *c* axis is significantly more compressible than *a*. Furthermore, the *B* tetrahedron is rigid whereas the eight-coordinated *A* polyhedron compresses significantly. A significant difference between the $A^{3+}B^{5+}O_4$ compounds and the $A^{2+}B^{6+}O_4$ tungstates and molyb-

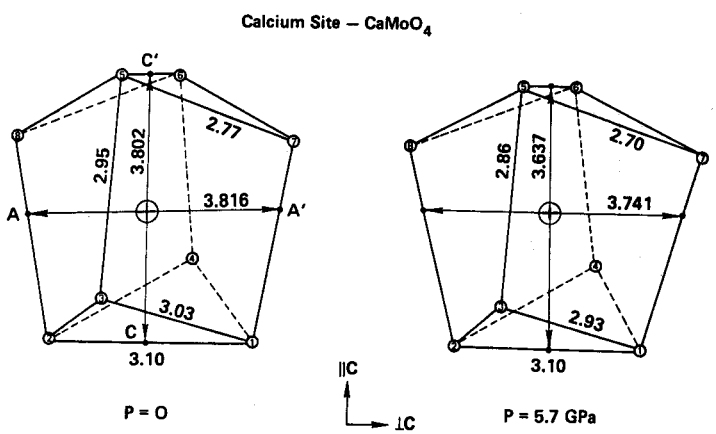


Fig. 5. Compression of the eight-coordinated polyhedron in $CaMoO_4$ between room pressure and 5.7 GPa. The tetragonal *c* axis is vertical. Segment *A*–*A'* represents the site width perpendicular to *c*; segment *C*–*C'* represents the site height parallel to *c*. Site compression along *C*–*C'* is approximately twice that along *A*–*A'*.

Table 6. Calcium site bond distances, adjacent O—Ca—O angles, polyhedral volume, and compressibilities for $CaWO_4$ and $CaMoO_4$

| Specimen | Pressure (GPa) | Ca-O[4]* | Ca-O[4] | O-O[4]† | O-O[4] | O-O[4] | O-O[2] | O-Ca-O[4] | O-Ca-O[4] | O-Ca-O[4] | O-Ca-O[2] | Volume (Å$^3$) |
|---|---|---|---|---|---|---|---|---|---|---|---|---|
| $CaWO_4$ | 0.0001 | 2.441(5)‡ | 2.478(5) | 2.770(3) | 2.938(2) | 3.040(10) | 3.139(10) | 68.6(1) | 73.3(1) | 76.3(2) | 80.0(2) | 26.4(1) |
| | 0.0001 in cell | 2.378(23) | 2.496(15) | 2.734(16) | 2.941(3) | 2.969(26) | 3.085(21) | 68.2(4) | 74.2(3) | 75.0(5) | 80.9(10) | 25.3(2) |
| | 1.03(5) | 2.370(21) | 2.484(13) | 2.720(15) | 2.924(3) | 2.962(23) | 3.081(19) | 68.1(4) | 74.1(2) | 75.2(5) | 81.1(9) | 25.4(2) |
| | 2.03(5) | 2.345(19) | 2.470(13) | 2.695(13) | 2.904(3) | 2.922(21) | 3.081(17) | 68.0(3) | 74.1(2) | 74.7(4) | 82.1(8) | 24.7(1) |
| | 3.12(5) | 2.331(23) | 2.464(15) | 2.683(15) | 2.890(4) | 2.912(26) | 3.068(21) | 68.0(4) | 74.1(3) | 74.7(5) | 82.3(10) | 24.4(2) |
| | 4.09(5) | 2.339(23) | 2.426(15) | 2.694(17) | 2.873(3) | 2.881(26) | 3.035(21) | 68.8(4) | 74.2(3) | 74.4(5) | 80.9(10) | 24.0(2) |
| | Compressibility ($GPa^{-1}$) | 0.005(1) | 0.006(1) | 0.004(1) | 0.0056(2) | 0.007(1) | 0.003(1) | | | | | 0.014(6) |
| $CaMoO_4$ | 0.0001 | 2.450(3) | 2.465(3) | 2.774(2) | 2.952(1) | 3.032(6) | 3.101(6) | 68.7(1) | 73.8(1) | 76.2(1) | 78.5(1) | 26.4(1) |
| | 1.30(5) | 2.431(11) | 2.447(7) | 2.759(8) | 2.935(2) | 2.994(14) | 3.079(11) | 68.9(2) | 74.0(1) | 75.7(3) | 78.6(4) | 25.8(1) |
| | 2.49(5) | 2.427(7) | 2.431(4) | 2.751(6) | 2.916(1) | 2.986(8) | 3.079(6) | 69.0(1) | 73.8(1) | 75.8(2) | 78.7(3) | 25.5(1) |
| | 3.65(5) | 2.398(8) | 2.421(5) | 2.725(6) | 2.894(1) | 2.949(9) | 3.074(7) | 68.9(1) | 73.8(1) | 75.4(2) | 79.7(3) | 24.8(1) |
| | 4.19(5) | 2.393(11) | 2.413(7) | 2.720(8) | 2.884(2) | 2.939(14) | 3.068(11) | 69.0(2) | 73.8(2) | 75.4(3) | 79.7(4) | 24.6(1) |
| | 5.10(5) | 2.386(12) | 2.399(8) | 2.705(21) | 2.867(2) | 2.919(16) | 3.094(13) | 68.8(2) | 73.6(2) | 75.2(3) | 80.8(5) | 24.3(1) |
| | 5.71(5) | 2.389(14) | 2.396(9) | 2.704(10) | 2.859(3) | 2.933(18) | 3.098(15) | 68.8(2) | 73.4(2) | 75.6(4) | 80.9(6) | 24.2(1) |
| | Compressibility ($GPa^{-1}$) | 0.0050(5) | 0.0050(2) | 0.0045(3) | 0.0055(2) | 0.0068(6) | 0.0012(8) | | | | | 0.015(1) |

*Bracketed figures represent bond multiplicities.
†Shared edge.
‡Parenthesized figures represent esd's.

dates, however, is the magnitude of these changes with pressure. Bulk moduli of $BiVO_4$ and $LaNbO_4$ are 130 and 150 GPa, respectively, whereas bulk moduli of the tungstates and molybdates are only 70–100 GPa. These differences in bulk moduli are a consequence of different compressibilities of the eight-coordinated polyhedra.

Polyhedral compressibility is proportional to polyhedral volume divided by cation formal charge [12]. The most compressible ionic clusters are thus large alkali cation polyhedra, such as those found in the alkali scheelites (e.g., $NaReO_4$ and $KRuO_4$). Compounds of the type $A^{2+}B^{6+}O_4$, such as the tungstates and molybdates, will be significantly less compressible than alkali scheelites, and the compounds with trivalent $A$ cations, including $Bi^{3+}$ and $La^{3+}$, will be even less compressible. The least compressible scheelite-type compounds will be of the type $A^{4+}B^{4+}O_4$, including $ZrGeO_4$ and, perhaps, high-pressure modifications of some silicates. In all these scheelite-type compounds it is expected that the $B$ tetrahedra will behave as rigid structural elements; it is compression of $A-O$ bonds that will determine the magnitude of the bulk modulus.

### *Structurally controlled $ABO_4$ phase transitions*

The stable structure type of $ABO_4$-type compounds is controlled, in large measure, by the cation radius ratios of $A$ to $B$ [9, 22]. Compounds of the type $AWO_4$ and $AMoO_4$, for example, occur in the scheelite form if the radius of $A$ is greater than about 0.90 Å, but in the wolframite structure if the radius of $A$ is less than 0.90. Changes in temperature, pressure, or $A$-site composition do not significantly alter the size of the W or Mo tetrahedron, but do cause changes in the effective radius of the eight-coordinated cation. It is thus possible, by judicious selection of $A$-site composition, to synthesize tungstates or molybdates that are close to the scheelite–wolframite type transition under room conditions of temperature and pressure [21]. Compounds of these critical compositions could prove useful in elucidating the mechanisms of transition between the similar, but topologically distinct, scheelite and wolframite structures.

*Acknowledgements*—The authors gratefully acknowledge the contributions of A. Jayaraman, G. Muncill, D. Virgo and H. S. Yoder, Jr., who reviewed this paper. This work was supported by National Science Foundation grant EAR81-15517.

## REFERENCES

1. Nicol M. and Durana J. F., *J. Chem. Phys.* **54,** 1436 (1971).
2. Ganguly B. N. and Nicol M., *Phys. Status Solidi* **B79,** 617 (1977).
3. Breitinger D. K., Emmert L. and Kress W., *Ber. Bunsenges. Phys. Chem.* **85,** 504 (1981).
4. Jayaraman A., Batlogg B. and Van Uitert L. G., *Phys. Rev. B* **28,** 4774 (1983).
5. Wada M., Nakayama Y., Sawada A., Tsunekawa S. and Ishibashi Y., *J. Phys. Soc. Japn* **47,** 1575 (1979).
6. Hazen R. M. and Mariathasan J. W. E., *Science* **216,** 991 (1982).
7. Fonteneau G., L'Helgoualch H. and Lucas J., *Rev. Chim. Mineral.* **16,** 89 (1979).
8. Jayaraman A., private communication.
9. Sleight A. W., *Acta Crystallogr.* **B28,** 2899 (1972).
10. King H. and Finger L. W., *J. appl. Crystallogr.* **12,** 374 (1979).
11. Finger L. W., Hadidiacos C. G. and Ohashi Y., *Carnegie Inst. Washington Yearb.* **72,** 694 (1973).
12. Hazen R. M. and Finger L. W., *Comparative Crystal Chemistry.* Wiley, New York (1982).
13. Piermarini G. J., Block S., Barnett J. D. and Forman R. A., *J. appl. Phys.* **46,** 2774 (1975).
14. Piermarini G. J., Block S. and Barnett J. D., *J. appl. Phys.* **44,** 5377 (1973).
15. Hamilton W. C., *International Tables for X-Ray Crystallography,* Vol. 4, p. 273. International Union of Crystallographers, Birmingham, England (1974).
16. Finger L. W. and King H., *Am. Min.* **63,** 337 (1978).
17. Farley J. M., Saunders G. A. and Chung D. Y., *J. Phys. C* **8,** 780 (1975).
18. Robinson K., Gibbs G. V. and Ribbe P. H., *Science* **172,** 567 (1971).
19. Hazen R. M. and Finger L. W., *J. Geophys. Res.* **84,** 6723 (1979).
20. Deshpande V. T. and Suryanarayana S. V., *J. Phys. Chem. Solids* **30,** 2484 (1969).
21. Mariathasan J. W. E., Ferroelastic transitions in scheelite crystals. Ph.D. thesis, Oxford University (1983).
22. Fukunaga O. and Yamaoka S., *Phys. Chem. Min.* **5,** 167 (1979).